ANALYSIS OF PERFORMANCE OF DIFFERENT NUMERICAL METHODS TO CAPTURE THE SCALE EFFECT

Ignacio Iturrioz
Programa de Pós Graduação em Engenharia Mecânica (PROMEC) - Universidade Federal do Rio Grande do Sul (UFRGS)
Osvaldo Aranha, 99 3 andar – CEP 90035-190 – Porto Alegre – RS – Brasil
e-mail: Ignacio@mecanica.ufrgs.br

Virginia Maria Rosito d'Ávila
Programa de Pós Graduação em Engenharia Civil (PPGEC) - Universidade Federal do Rio Grande do Sul (UFRGS)
e-mail: vichy@ufrgs.br

Eduardo Bittencourt
Programa de Pós Graduação em Engenharia Civil (PPGEC) - Universidade Federal do Rio Grande do Sul (UFRGS)
e-mail:bittenco@cpgec.ufrgs.br

Atilio Morquio
Instituto de Estruturas e Transportes, Universidade de la Republica, Montevideo Uruguay
e-mail: Atilio@fing.edu.uy

Abstract. *The study of scale effect has puzzled researchers since the beginning of modern science. Galileo and Leonardo da Vinci already had discussed the subject in their work. Another phenomenon that has important influence on mechanical properties of the materials is the strain velocity of the applied load. Although many aspects may be investigated, it is clear that characteristic dimensions and wave velocities of the material have a key hole. To take into account these effects is fundamental when problems of fracture and fragmentation are studied. To formulate a scale law, the proposition presented by Morquio and Riera (2004) will be used. The numerical methods in general consider, implicitly or explicitly, the existence of the above mentioned material characteristics. In this context different numerical methodologies are explored here. In the present paper is first shown the theoretical framework proposed by Morquio and Riera to represent the scale law. Then a brief description about the three numerical methodologies analyzed and the determination of adimensional parameters is briefly explained. Finally a comparison in terms of characteristic length and strain rate, that leads to a scale law in each method is presented and a discussion about the physical significance of these parameters is pointed out.*

Keywords: *Scale Effect, Strain velocity dependence, Fracture Mechanics, Numeric Simulation.*

1. Introduction

For structural design, the knowledge about material properties in the real structure dimensions and the applied strain rate level are of fundamental importance. Generally the real structure material properties are different from those in a simple test specimen because exists the interaction between the material properties and the following factors: (i) structure size, (ii) strain rate applied on it. The material properties interaction with the size structure (size effect) has been studied since the modern science beginning - the Leonardo and Galileo works are evidence of that. Presently the models created by Bazant and Chen (1997) and Carpinteri et al (1995) are examples of recent studies that have been generated in the size effect area. In Latin-America, is relevant to mention the work of Morquio and Riera (2004) which showed a theoretical framework that permitted include the different size law models considering not only the size effect but also the strain rate dependencies.

The present paper is organized in the following way. In section 2 is shown the theoretical framework proposed by Morquio and Riera (2004) to represent the scale law. Then, in section 3, a brief description about the three numerical methodologies analyzed: the discrete element method (DEM) proposed by Rocha (1989), the finite element method considering cohesive interfaces (IC-FEM) originally developed by Needleman (1987), and the smeared crack method (SF-FEM) due to Rots (1988). The determination of adimensional parameters is briefly explained in sections 4 and 5. Finally, in section 6, comparisons in terms of characteristic lengths and strains rate, that lead to a scale law in each method is presented and the discussion about the physical significance of these parameters is pointed out.

2. Characteristic Length and Strain Velocities

The scale effect is generally studied for a determined structure response, that here is generically named with the letter *Y*. This response can be, for example, the material nominal strength, the maximum storage elastic energy before fracture, etc. By comparing the results obtained in different size structures with geometric similarities, the scale effect can be verified.

Two structures (*a* e *b*) are considered geometrically similar when the quotients between dimensions ($d_b / d_a = \lambda$) are a constant, for any selected structural dimension. Obviously the obtained responses (Y_a, Y_b, ...) might be or not different for the different sizes of the structure. In the first case ($Y_b = Y_a = ... =$ constant), does not exist a scale effect, and the structural response is independent of the structure size. In the other case *($Y_b \neq Y_a \neq ...$),* the response is function of the structure size and consequently does exist a scale effect. An example of this scale effect is the microstructure size of grains in metals. It is known that the smaller the grain size, the harder the metal.

Consider that the response *Y* for a structure with a geometric dimension *d* is defined by a scale law function *f* as:

$$Y = Y_a f(\lambda) \tag{1}$$

where $\lambda = d / d_a$, and Y_a is a response for the structure that has the reference size d_a and *f* is an adimensional function that fulfill the condition $f(1) = 1$. If function *f* depends on the reference size d_a, it means that exists a material characteristic length (MCL). On the other hand, if function *f* is not dependent on d_a,, then does not exist a MCL. As stated by Bazant and Chen (1997), when does not exist a MCL, it is possible verify that *f* has the following form:

$$f(\lambda) = \lambda^m \tag{2}$$

The expression (2) represents the most generic form for the scale law, if does not exist a MCL. In this equation *m* represents any real number. If we consider that exists two MCL (c_1 e c_2) the response *Y* of the structure with geometric dimension *d* can be expressed in the form:

$$Y = Y_a f(\lambda, \mu, \eta) \tag{3}$$

where the adimensional parameters are: $\lambda = d / d_a$, $\mu = c_1 / d_a$ and $\eta = c_2 / d_a$. The function *f* must fulfill the condition: $f(1, \mu, \eta) = 1$, for any μ and η. Therefore when exist two or more characteristic lengths (c_1, c_2, ...) the function *f* must be independent of the selected reference dimension d_a, and will only depend on its characteristic lengths.

In a similar way, it is possible to define a material characteristic strain rate (MCSR), that arises when the structures responses due to loads with different strain rate applied are different. If a structure have two MCL and two MCSR the responses for two geometric dimensions Y_a and Y are defined as: Y_a => structural response with size d_a and strain rate $d\varepsilon_a/dt$; Y => structural response with size *d* and strain rate $d\varepsilon/dt$.

If we name c_1 and c_2 the MCLs and $d\varepsilon_{c1}/dt$, $d\varepsilon_{c2}/dt$ the MCSRs, the adimensional parameters should be defined as:

$$\lambda = d / d_a, \ \mu = c_1 / d_a, \ \eta = c_2 / d_a, \ \theta = \frac{d\varepsilon}{dt} / \frac{d\varepsilon_a}{dt}, \ \pi = \frac{d\varepsilon_{c1}}{dt} / \frac{d\varepsilon_a}{dt}, \ \gamma = \frac{d\varepsilon_{c2}}{dt} / \frac{d\varepsilon_a}{dt} \tag{4}$$

In this conditions, is possible to write:

$$Y = Y_a f(\lambda, \mu, \eta, \theta, \pi, \gamma) \tag{5}$$

3. The Numerical Methods Description

In the present section will be shown the main characteristics of the three different methods mentioned in the introduction: DEM (Rocha 1989), FEM-IC (Nedeelman 1987) and FEM-SF (Rots 1988).

3.1 The Discrete Element Method (DEM)

The DEM essentially consists in representing the continuum domain through regular array of truss bars as shown in Fig. 1, where group-working bar rigidity is equivalent to the mechanical behavior of the continuum domain in analysis. The elemental constitutive law represents the material non-linear behavior.

In Rocha (1989) an elemental bilinear constitutive law is proposed. This law captures the material behavior until the rupture and is based in the original idea presented by Hillerborg et al (1976). The constitutive law is given in terms of force and strain.

In the Fig. 1(c), P_{cr} represents the maximum tensile transmitted bar force and ε_p the associate strain with P_{cr}; E_A is the cubic model bar rigidity and k_r is the factor that is related to ductility (this parameter permits to calculate the strain where the bar stop transmitting tensile force, $\varepsilon_r = k_r \varepsilon_p$). The limit strain ε_r must permit that the area in Fig. 1(c) multiplied by the bar length L_{ele} be equal the available fracture energy *($Gf A_f$)* in the bar, where *Gf* is the specific fracture energy, and A_f is the fracture area that each bar represent.

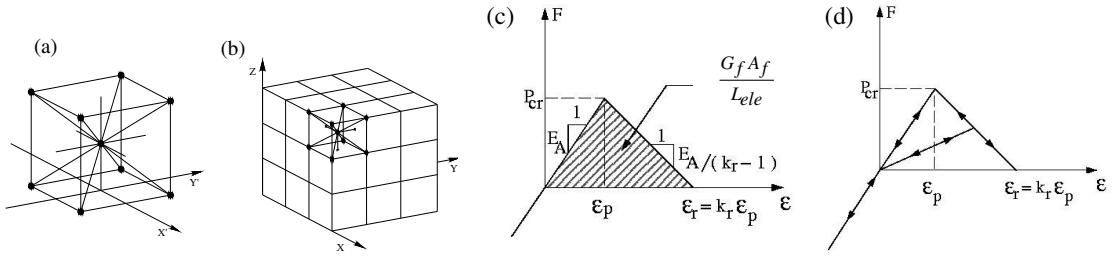

Figura 1 a) Cubic Module . b) Prism formed with several cubic Modules,
c) Uniaxial constitutive law, d) Charge and discharge scheme.

As the material has a brittle behavior, the linear fracture mechanics can be applied. The toughness can be expressed in terms of the Irwin stress intensity factor *(K_{Ic})* or in terms of the specific fracture energy *(G_f),* then it is possible to write

$$K_{IC} = \chi \cdot \sigma_t \cdot \sqrt{a} \qquad \text{and} \qquad G_f = \frac{K_{IC}^2}{E} \tag{6}$$

where χ is a parameter that depends on the problem geometry and a is the crack length. If the material behavior is linear up to rupture ($\sigma_t = \varepsilon_p E$), the critical strain is given by:

$$\varepsilon_p = R_f \cdot \left[\frac{G_f}{E \cdot}\right]^{1/2} \qquad \text{where} \qquad R_f = \frac{1}{\left(\chi \cdot \sqrt{a}\right)} \tag{7}$$

and R_f is a fail factor. This factor permits to introduce information about the intrinsic form of material rupture. The motion equations for the spatial discretization can be written as:

$$M \cdot \ddot{u} + f(t) = q(t) \tag{8}$$

In the equation (8), M represents the diagonal mass matrix proportional to the density ρ, u is the nodal displacement vector, $f(t)$ is the nodal internal force vector, $f(t)$ depends on previous and present displacements, and $q(t)$ is the nodal external applied force vector. As in elastic linear system, $f(t)=Ku(t)$, where K is the rigidity matrix. In systems with viscous forces, $f(t) = K \cdot u + C \cdot \dot{u}$. Considering the damping coefficient C proportional to the mass, $C=MD_f$, with D_f a constant that depends on the material and on the structure system. The motion Eq. (8) can be integrated numerically in the time domain with a explicit scheme (central difference methods).

It is important to point out that P_{cr}, ε_P, ε_r, G_f ,R_f,E, ρ, D_f, are exclusively material properties while A_f and L_{ele} are exclusively related to the numerical model. Parameters E_A and k_r are function of both model and material. This method was successfully used in the modeling of concrete, soils and other composite materials such as is shown in Riera and Iturrioz (1995) , Spellmeyer et al (2001), Barrios D'Ambra et al (2003).

3.2. The interface cohesive formulation (FEM-IC)

In the cohesive interface method, Finite Element nodes are linked by springs at the nodes in order to simulate crack opening. The relationship between normal stress (T_n) and displacement (Δ_n) for the springs is given below, see Needleman (1987) (observe that the spring displacement corresponds to crack opening.).

$$T_n = -\frac{G_f \Delta_n}{\delta_n^2} \exp\left(-\frac{\Delta_n}{\delta_n}\right) \tag{9}$$

The Fig. 2 shows the relation T_n versus Δ_n. Therefore an exponential law is considered, that reaches a peak stress values (σ_{max}) for an opening δ_n. (The above equation is valid if mode II of rupture is not present in the analysis). The area below this curve is equal to G_f, as can be easily observed integrating Eq. (9) in Δ_n from zero to infinity. In practice for an opening $\Delta_n \cong 5\delta n$ the whole fracture energy is consumed and rupture can be assumed. This value is denoted Δ^*_n.

From stress analysis in the crack tip, it is known that: $\sigma_{max} \cong 3.5\ \sigma_e$ for a plastic material ((σ_e), is the yield or flow stress), or, for an elastic material, $\sigma_{max} \cong E/10$, where E is the elastic modulus.

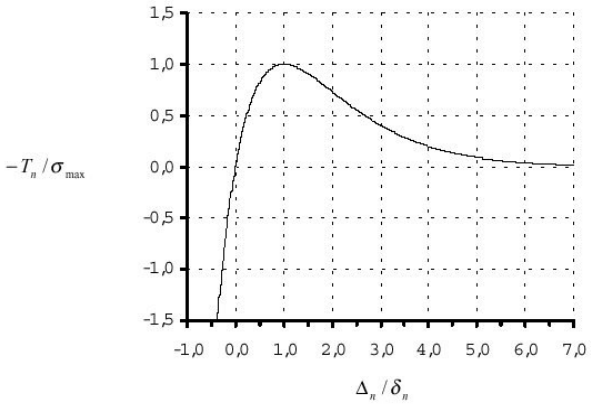

Figure 2: The normalized relationship between normal stress (T_n) and displacement (Δ_n).

The interface properties are linked though Eq.(10), that comes out from Eq.(9) for $\Delta_n = \delta_n$:

$$\delta_n = G_f / (\exp[1]\sigma_{max}) \tag{10}$$

The constitutive law of the elements linked by the interface function expressed in Eq.(9) can be of any type, but for the present study a linear elastic (Hooke) law, with E as the elastic modulus, was considered. Also the mass is considered uniformly distributed and characterized by a density ρ.

3.2. The smeared crack implementation (FEM-SF)

In smeared crack models, the discontinuity in the displacement field caused by the crack is smeared along the element, which has its constitutive relation changed (d´Avila (2003) and Rots (1988)).

A linear elastic behavior is considered for the uncracked material as much in compression as in tension. Fig. 3(a) represents the tension behavior until the maximum stress (σ_t) is reached.

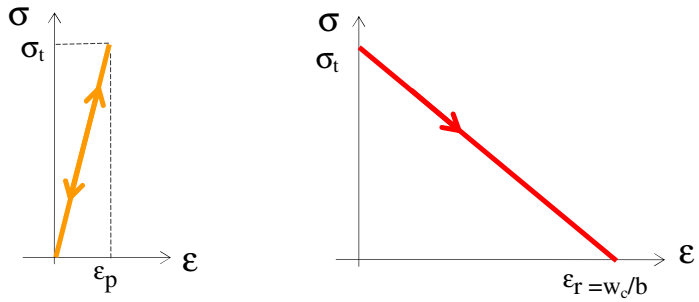

Figure 3: Constitutive relations: (a) uncracked material, (b) cracked material

Figure 3(b) shows the "stress x strain" cracked material softening behavior curve. The softening branch slope is dependent of the value ε_r, the maximum strain that allows traction transference between crack faces. The value of ε_r, is

$$\varepsilon_r = 2G_f/(\sigma_t b) \tag{11}$$

where b is the cracked zone dimension (cracked band). Observe that, as was indicated in Fig.3(b), $\varepsilon_r = w_c/b$, where w_c is the crack opening where the material do not transmit more tension (Hillerborg 1976). The softening branch slope results then dependent of the value of the cracked band b, since σ_t and G_f are material characteristic values.

The crucial point of the model is the correct determination of the crack band dimension value, since this value changes significantly the structural global response.

For isoparametric finite elements, Rots (1988) suggests the expressions below to conect L_{ele} with the crack band dimension in numerical simulations:

$$L_{ele} = b/\sqrt{2} \quad \text{(a)} \qquad L_{ele} = b \quad \text{(b)} \tag{12}$$

where L_{ele} is the dimension of the element in the cracked zone. Eq.12(a) is applied to four nodes elements with 2x2 gauss points and Eq. 12(b) for eight nodes elements with 3x3 gauss points.

4. The Scale Laws Studied

In the present section, the methodology to identify the parameters of the scale law is shown. In all cases studied, the Poisson coefficient is maintained constant and in this manner the number of involved parameters is reduced.

The following magnitude nomenclature will be utilized : **M:** Mass magnitude, **L**: Length magnitude, **T**: Time magnitude. As an example, the dimensional analysis by DEM case is shown. In this case the following input parameters are used:

a) E = Elasticity Modulus,**[ML^{-1} T^{-2}]**
b) ρ = Density, **[ML^{-3}]**
c) G_f = Especific Fracture Energy, **[MT^{-2}]**
d) R_f = fail factor, **[L$^{-1/2}$]**
f) D_f = damping factor, **[T^{-1}]**

Comparing the results Y_a and Y that correspond to two structures (composed with the same material and different sizes, but geometrically similar to each other, submitted to different strain rate). In addition to the material property parameters, the following variables will enter in the analysis:

i) da =the first structure size**, [L]**
j) d = the second structure size, **[L]**
k) $d\varepsilon_a/dt$ = the applied strain rate to the first structure**, [T^{-1}]**
l) $d\varepsilon/dt$ = the applied strain rate to the second structure**, [T^{-1}]**

In the DEM analysis, the bar length (L_{ele}) was maintained constant for all case simulated. Then L_{ele} does not entry as an input parameter. Consequently it is possible to write:

$$Y = F(E, \rho, G_f, R_f, D_f, d, \frac{d\varepsilon}{dt}) \quad \text{(a)}, \qquad Y_a = F(E, \rho, G_f, R_f, D_f, d_a, \frac{d\varepsilon_a}{dt}) \quad \text{(b)} \tag{13}$$

And the quotient of both responses will be:

$$\frac{Y}{Y_a} = F^*(E, \rho, G_f, R_f, D_f, d, d_a, d\varepsilon/dt, d\varepsilon_a/dt) \tag{14}$$

The quotient of Eq. (14) can be expressed in terms of products of the power of input parameters. It must be accomplish that:

$$E^{a1} \times \rho^{a2} \times {G_f}^{a3} \times {R_f}^{a4} \times {D_f}^{a5} \times d^{a6} \times {d_a}^{a7} \times \left(\frac{d\varepsilon}{dt}\right)^{a8} \times \left(\frac{d\varepsilon_a}{dt}\right)^{a9} = \text{adimensional} \tag{15}$$

and, consequently:

$$\begin{aligned} &a_1 + a_2 + a_3 = 0 \ \text{(for magnitude } \mathbf{M}) \\ &a_1 + 3a_2 + a_4/2 - a_6 - a_7 = 0 \ \text{(for magnitude } \mathbf{L}) \\ &2a_1 + 2a_3 + a_5 + a_8 + a_9 = 0 \ \text{(for to magnitude } \mathbf{T}) \end{aligned} \tag{16}$$

Using the Eq. (16) is possible eliminate a_1, a_7 and a_9 and to obtain that:

$$\left(\frac{\rho(d\varepsilon_a/dt)^2 {d_a}^2}{E}\right)^{a2} \times \left(\frac{G_f}{E d_a}\right)^{a3} \times \left(R_f {d_a}^{1/2}\right)^{a4} \times \left(\frac{D_f}{d\varepsilon_a/dt}\right)^{a5} \times \left(\frac{d}{d_a}\right)^{a6} \times \left(\frac{d\varepsilon/dt}{d\varepsilon_a/dt}\right)^{a8} = \text{adimensional} \tag{17}$$

Equation (14) can be then rewritten as:

$$\frac{Y}{Y_a} = f(\lambda, \mu, \eta, \theta, \pi, \gamma) \tag{18}$$

$$\lambda=\frac{d}{d_a},\mu=\frac{R_f^{-2}}{d_a}=\frac{c_1}{d_a},\eta=\frac{G_f}{Ed_a}=\frac{c_2}{d_a},\theta=\frac{d\varepsilon/dt}{d\varepsilon_a/dt},\gamma=\frac{R_f^{\ 2}}{d\varepsilon_a/dt}\sqrt{\frac{E}{\rho}}=\frac{d\varepsilon_{c1}/dt}{d\varepsilon_a/dt}\pi=\frac{D_f}{d\varepsilon_a/dt}=\frac{d\varepsilon_{c2}/dt}{d\varepsilon_a/dt} \tag{19}$$

From nine variables illustrated in Eq. (14), five were material function (E,ρ,G_f,R_f,D_f), two were structure dimensions function (d,d_a) and two were function of the applied strain rate ($d\varepsilon/dt$, $d\varepsilon_a/dt$). This input variables define the studied problem in DEM and were reduced to six adimensional parameters illustrated in Eq. (18). In this case four parameters define the material properties (μ,η,π,γ), one the structure dimensions (λ) and one the applied strain rate (θ).

In the case of FEM-IC the response quotient used is presented as follow:

$$\frac{Y}{Y_a}=F^*(E,\rho,G_f,\delta_n or\sigma_{\max},\Delta_n^*,d,d_a,\frac{d\varepsilon}{dt},\frac{d\varepsilon_a}{dt}) \tag{20}$$

resulting

$$\frac{Y}{Y_a}=f(\lambda,\mu,\eta,\theta,\tau,\gamma) \tag{21}$$

$$\lambda=\frac{d}{d_a},\mu=\frac{\delta_n}{d_a}or\frac{G_f}{\sigma_{\max}d_a}=\frac{c_1}{d_a},\eta=\frac{G_f}{Ed_a}=\frac{c_2}{d_a},\theta=\frac{\frac{d\varepsilon}{dt}}{\frac{d\varepsilon_a}{dt}},\tau=\frac{\Delta_n^*}{d_a}=\frac{c_3}{d_a},\gamma=\frac{\frac{1}{\delta_n}}{\frac{d\varepsilon_a}{dt}}\sqrt{\frac{E}{\rho}}=\frac{\frac{d\varepsilon_{c1}}{dt}}{\frac{d\varepsilon_a}{dt}} \tag{22}$$

Finally for FEM-SF is possible to write

$$\frac{Y}{Y_a}=F^*(E,G_f,\sigma_t,b,d,d_a,\frac{d\varepsilon}{dt},\frac{d\varepsilon_a}{dt}) \tag{23}$$

or

$$\frac{Y}{Y_a}=f(\lambda,\mu,\eta,\tau)\ \text{(a)}\quad \text{with}\ \lambda=\frac{d}{d_a},\mu=\frac{G_f}{\sigma_t d_a}or\frac{w_c}{d_a}=\frac{c_1}{d_a},\eta=\frac{G_f}{Ed_a}=\frac{c_2}{d_a},\tau=\frac{b}{d_a}=\frac{c_3}{d_a}\quad \text{(b)} \tag{24}$$

Table 1. Input Data and Scale Law Characteristic Parameter for FEM-IC, FEM-SF and DEM

Input Data	**Var_1[$ML^{-1}T^{-2}$]**	**Var_2 [ML^{-3}]**	**Var_3[MT^{-2}]**	**Var_5**	**Var_6**
DEM	E	ρ	G_f	R_f **[L-1/2]**	D_f [T^{-1}]
FEM-IC	E	ρ	G_f	δ_n **[L]** or σ_{max} [$ML^{-1}T^{-2}$]	Δ_n* [L]
FEM-SF	E	–	G_f	σ_t[$ML^{-1}T^{-2}$] or w_c **[L]**	b [L]
Characteristic parameters	c_1 **[L]**	c_2 **[L]**	c_3 **[L]**	$d\varepsilon c_1/dt$ [T^{-1}]	$d\varepsilon c_2/dt$ [T^{-1}]
DEM	$1/R_f^2$	G_f/E	-	$R_f^2\ (E/\rho)^{0.5}$	D_f
FEM-IC	δn or G_f/σ_{max}	G_f/E	Δ_n*	$1/\delta n\ (E/\rho)^{0.5}$	-
FEM-SF	$G_f/\sigma t$ or $w_c/2$	G_f/E	b	-	-

As much in FEM-IC as in FEM-SF was considered that the mesh size L_{ele} changes proportionally with the structure geometry. In other words *(L_{ele}/d =Constant)*. For this reason L_{ele} is not considered as an input independent variable, the study of L_{ele} influence will be object of a future work.

In Table 1 is illustrated the independent input variables and the characteristic values for the three analyzed methods (DEM, FEM-IC, FEM-SF) to facilitate the comparison between them.

5. Verification Methodology to test the analyzed Algorithms

In order to compare the different algorithms, four simulations with responses Y_1, Y_{a1}, Y_2 and Y_{a2}, are considered. The following conditions are accomplished:

a) The magnitudes that define the material properties are equal for the two first cases (1, *a*1) and for the last two cases (2, *a*2), although not necessarily equal between them.
b) The quotients between the sizes d_1/d_{a1} and d_2/d_{a2} are equal.
c) The quotients between the strain rates $\frac{d\varepsilon_1}{dt}/\frac{d\varepsilon_{a1}}{dt}$ and $\frac{d\varepsilon_2}{dt}/\frac{d\varepsilon_{a2}}{dt}$ are equal.
d) The adimensional parameters of the two first cases (1, a1) are equal to the two last cases (2, *a*2).

If the four conditions are fulfilled it is possible to say that:

$$Y_1 / Y_{a1} = Y_2 / Y_{a2} \tag{25}$$

For the DEM, Eq. (25) results:

$$\frac{Y_1}{Y_{a1}} = f(\lambda_1,\mu_1,\eta_1,\theta_1,\pi_1,\gamma_1) = \frac{Y_2}{Y_{a_2}} = f(\lambda_2,\mu_2,\eta_2,\theta_2,\pi_2,\gamma_2) \text{ where } \lambda_1=\lambda_2,\mu_1=\mu_2,\eta_1=\eta_2,\theta_1=\theta_2,\pi_1=\pi_2,\gamma_1=\gamma_2 \tag{26}$$

The same idea can be applied to the FEM-IC and the FEM-SF. In order to verify that DEM, FEM-IC and FEM-SF accomplish the scale law, four cases were simulated in each method. This verification for the DEM was shown in Morquio et al (2004), and for the others two methods are been presented in d'Avila (2005). These verifications were done in terms of rupture strength, strains, maximum elastic strain energy storage in the structure, etc, with notably precision.

6. Discussion and Conclusions

In the present work the formulation development by Morquio and Riera (2004) was applied to formulate a scale law in terms of adimensional variables for three fracture mechanics algorithms (DEM, FEM-IC, FEM-SF).

Trying to understood the physical meaning of characteristic parameters shown in Table 1, the following equivalencies are used:

$$G_f, K_{IC} = \frac{\sigma_t}{Rf}, G_f = \frac{K_{IC}^2}{E}, \sigma_t = E\varepsilon_p, G_f = \frac{w_c\sigma_t}{2} \tag{27}$$

It can be observed that:

a) Using the Eq. (27), the characteristic lengths c_{1DEM}, $c_{1FEM\text{-}IC}$, $c_{1FEM\text{-}SF}$ shown in Table 1, can be expressed as:

$$c_{1DEM} = \frac{1}{Rf^2} = \frac{G_f}{E\varepsilon_p^2} \text{ (a)}, \qquad c_{1FEM-SF} = \frac{G_f}{\sigma_t} = \frac{G_f}{E\varepsilon_p} = \frac{w_c}{2} \text{ (b)}, \qquad c_{1FEM-IC} = \delta_n \;\; or \;\; c_{1FEM-IC}\frac{G_f}{\sigma_{\max}} \text{ (c)} \tag{28}$$

b) The second characteristic length $c_2=G_f/E$, as seen in Table 1, has the same value for the three methods. Trying to find a physical meaning for c_2, is carried out the following transformation in c_2 expression

$$c_2 = \frac{G_f}{E} = \frac{G_f}{E}\frac{((1/2)l_{crit}^3\varepsilon_p^2)}{((1/2)l_{crit}^3\varepsilon_p^2)} = \frac{G_f l_{crit}^2}{U}((1/2)l_{crit}\varepsilon_p^2) \tag{29}$$

If we interpret l_{crit} as the length of the side of a cube that for its critical strain ε_p storages a strain elastic energy U, equal to the necessary energy to break a area $(l_{crit})^2$, then is possible to re-write c_2 in terms to l_{crit} :

$$c_2 = G_f / E = ((1/2)l_{crit}\varepsilon_p^2) \tag{30}$$

c) The characteristic length c_1 can be written for DEM and FEM-SF in the following way:

$$c_1 = \frac{G_f}{E}\varepsilon_p^{\omega} = \frac{l_{crit}\varepsilon_p^{\omega+2}}{2} \tag{31}$$

where for DEM (ω=-2) and for FEM-SF(ω=-1) .

d) The characteristic length c_3, see (Table 1), only appears for (FEM-IC e FEM-SF) and it is linked to the shape of strain softening in the constitutive law used in each case.

e) Regarding the characteristic strain rates, it is possible to observe that in the FEM-SF this parameter does not appear because, in this case, the method uses a quasi-static analysis. Concerning DEM and for FEM-IC, $d\varepsilon c_1/dt$ presents an interesting similarity:

$$\left(\frac{d\varepsilon_{c1}}{dt}\right)_{DEM} = R_f^2\sqrt{\frac{E}{\rho}} \quad \text{(a)} \qquad \left(\frac{d\varepsilon_{c1}}{dt}\right)_{FEM-IC} = \frac{1}{\delta_n}\sqrt{\frac{E}{\rho}} \quad \text{(b)} \tag{32}$$

reminding that $(E/\rho)^{0.5}$ is a propagation dilatational wave speed in the elastic medium, it is possible to say that the inverse of the $d\varepsilon c_1/dt$ determine the time that the dilatational wave takes to cross the characteristic length c_1.

The DEM has another characteristic strain rate ($d\varepsilon c_2/dt$) linked to the viscous damping proportional to the structure mass (D_f).

f) Finally it is possible to consider the following equivalence between (DEM, FEM-IC, FEM-SF) for the characteristic length c_1 in terms of the intrinsic parameters of each method and for the l_{crit} previously defined in Eq.(30)

$$\delta_n \approx \frac{1}{Rf^2} \approx l_{crit} \approx w_c \tag{33}$$

As a final conclusion it is possible to say that the scale law analysis permits to infer fundamental information about the meaning of the parameters used by each method. The comparison among different methods gives a new light in the interpretation of these parameters.

7. Acknowledgements

The authors wish to acknowledge the partial contribution of CNPq, CAPES, FINEP and FAPERGS.

8. References

Barrios D'Ambra, R., Iturrioz, I., Fasce, L.A., Frontini, P. M., Cisilino, Adrián P., 2003, "Simulación numérica del ensayo de impacto en probetas de polímeros utilizando el método de los elementos discretos", Proceedings of CILAMCE 2003, Brasil.

Bazant, Z.P., Chen E.P., 1997, "Scaling of structural failure", Applied Mechanics review, Vol.50, No.10, p 593-627.

Carpinteri, A., Chiaia B., Ferro G., 1995, "Size effects on nominal tensile strength of concrete structures: multifractality of material ligaments and dimensional transition from order to disorder", Materials and Structures, 28 p 311-317.

d'Avila, V.M.R., 2003, "Estudo sobre Modelos de Fissuração de Peças de Concreto armado via método dos elementos finitos". Tese (Dsc. em Engenharia) – Programa de Pós-Graduação em Engenharia Civil, UFRGS, Porto Alegre.

d'Avila, V.M.R., Bittencourt, E., Iturrioz, I., Morquio, A., 2005 "Perfomance de diferentes Métodos Numericos en Capturar el Efecto de Escala, Parte II". Jornadas SAM/CONAMET, Nov. Mar del Plata, Argentina.

Hillerborg, A.; Modéer,M., Peterson, P.E., 1976 "Analysis of Crack Formation and Crack Growth in Concrete by Means of Fracture Mechanics and Finite Elements", Cemente and Concrete Reserch, Vol.6, p.773-782.

Morquio, A., Riera, J., 2004, "Size and strain rate effects in steel structures", Engineering Structures, Vol. 26, Issue 5, April, p 669-679.

Morquio, A., Iturrioz, I., Tesser, G., 2004 ,"Simulación del efecto de tamaño en acero y su interacción con la velocidad de deformación con la velocidad de deformación utilizando el metodo de los elementos discretos", ENIEF 2004, S. C. Bariloche , Argentina.

Needleman, A., 1987, "A continuum model for void nucleation by inclusion debonding", Journal of Applied Mechanics, Vol.54, p. 525-531.

Riera, J.D., Iturrioz, I., 1995 "Discrete element dynamic response of elastoplastic shells subjected to impulsive loading", Communications in Numerical Methods in Engineering, Vol. 11, p 417-426.

Rots, J.G., 1988 "Computational Modeling of Concrete Fracture", Doctoral Thesis, Delft University of Technology, Delft, Netherlands.

Rocha, M.M., 1989, "Ruptura e efeito de escala em materiais não homogêneos de comportamento frágil", Porto Alegre, 123 p. Dissertação (Mestrado), Curso de Pós-Graduação em Engenharia Civil, UFRGS.

Spellmeyer, T., Barrios D'Ambra, R., Iturrioz, I., 2001, "Simulación numérica de la propagación de fisuras en sólidos utilizando el método de los elementos discretos", In: ENIEF XII, Córdoba, Argentina. Mecánica Computacional Vol 20 p.506-513.

.

9. Responsibility notice

The authors are the only responsible for the printed material included in this paper.